Elementary local configurations, microscopic rules and Langevin equations for two models of molecular-beam epitaxy

1998 J. Phys. A: Math. Gen. 31 7211

(http://iopscience.iop.org/0305-4470/31/35/003)

J. Phys. A: Math. Gen. **31** (1998) 7211–7225. Printed in the UK PII: S0305-4470(98)90891-5

Elementary local configurations, microscopic rules and Langevin equations for two models of molecular-beam epitaxy

G Costanza

Departamento de Física, Laboratorio de Física de Superficies y Medios Porosos, Universidad Nacional de San Luis, Chacabuco 917, 5700 San Luis, Argentina

Received 20 January 1998, in final form 2 June 1998

Abstract. Stochastic Langevin equations for the Wolf–Villain (WV) and Das Sarma–Tamborenea (DT) models are derived using the alternative method recently developed by Costanza (1997 *Phys. Rev.* E **55** 6501) which avoids the complications arising in the calculation of the first moment of the transition rate required in the master equation approach. The calculations are compared with those recently published by Zhi-Feng Huang *et al* (1996 *Phys. Rev.* E **54** 5935) obtaining the same results, as is expected. The microscopic rules are derived from the set of 243 elementary local configurations needed for the description of these two models and after using simple summation rules these were reduced to 16 for the DT model and to 25 for the WV model. The number of microscopic rules needed for the description of the present models are considerably larger than the previously solved models.

1. Introduction

Surface growth via molecular-beam epitaxy is of great theoretical importance and has received much attention during recent years, particularly due to the technological implications. In order to describe the surface growth different models have been introduced in the literature [1–3]. Simulations are extensively performed in order to provide the scaling exponents [4, 5] but this approach has sometimes shown that the results obtained are doubtful and only careful studies can show to what universality classes the different models [6–12] belong. These problems and the obvious pure theoretical interest in the study of the universality classes via the construction of continuum growth equations largely justify the two known approaches to derive the Langevin equations [13, 14]. It is well known that the two most studied models of molecular-beam epitaxy are the Das Sarma–Tamborenea (DT) [4] and Wolf–Villain (WV) [5]. These models differ slightly from each other in the microscopic rules that define the relaxation process: in the former the particle may move to the nearest neighbour which increases its coordination number and in the latter towards the nearest-neighbour site which has the largest coordination number. The two known routes to derive stochastic Langevin equations are the evaluation of the first moment of the transition rate [13], or direct use of the microscopic rules describing the growth process [14]. The latter method has advantages over the master equation approach due to the more straightforward and intuitive nature of the procedure. Recently the two above-mentioned models were solved by the master equation approach by Zhi-Feng Huang *et al* [15] obtaining the corresponding Langevin equations.

0305-4470/98/357211+15$19.50

In this paper we will obtain both equations by use of the method developed by the author in [14]. For the sake of completeness and clarity, the general procedure described in section II of [14], is reviewed in section 2. The remainder of this paper is as follows. In section 3 the elementary local configurations used to derive the microscopic rules are defined and constructed for a simplified version of the DT model considering only the relaxation mechanism (previously solved in [14]) avoiding the complication arising when diffusion is also considered. In section 4 we describe the procedure leading to the Langevin equation corresponding to the DT model. In section 5 the WV model is analysed and finally conclusions are presented in section 6.

2. Discrete models and Langevin-type equations

Our procedure to obtain the Langevin equation for the motion of the surface profile is based on the elementary microscopic growth rules for the height of a given site. In the following we consider a one-dimensional lattice with N sites with periodic boundary conditions. The height of a given site i, $h_i(t_n)$ is a function of the index i and time t_n. One can specify the procedure as follows.

(i) A dummy index j is chosen at random from N integer numbers.

(ii) The height of a site i at time $t_{n+1} = t_n + \tau_0$ (here τ_0 is the elemental timestep between two successive depositions in any site of the lattice) is given by

$$h_i(t_{n+1}) = R_j(\{h_i(t_n)\}) \tag{1}$$

where $R_j(\{h_i(t_n)\})$ gives the growth rules for the height of the site i and depends on the value of the dummy index j. Such dependence is specified by the rules '*a priori*', and in general can be dependent on the complete set of heights $\{h_i(t_n)\}$ at time t_n before deposition.

Let us define now the time interval between two successive depositions on site i as

$$\tau_{i,m} = \tau + \delta\tau_{i,m} \tag{2}$$

where τ is the mean time interval between two successive depositions on site i and $\delta\tau_{i,m}$ is the random deviation from the mean value τ. With this consideration we can write equation (1) for time $t + \tau_{i,m}$ as

$$h_i(t + \tau_{i,m}) = R_j(\{h_i(t + \tau_{i,m} - \tau_0)\}) \tag{3}$$

where $t = t_m$ is the time of the previous deposition (see figure 1).

In order to illustrate the derivation of the Langevin equation from the growth rules given in equation (3), in sections 4 and 5 we shall obtain the microscopic rules for two well known growth models: the DT and the WV models.

3. Elementary local configurations

In order to obtain the microscopic rules that define each model it is necessary to generate all the possible 'local configurations' according to the specific model. We shall see that the number of local configurations that define a model are in general greater then, or at least equal to, the number of microscopic rules. To generate the possible local configurations the following steps are necessary: (i) determine the maximum number of neighbours involved in the growth of one site corresponding to a given model, (ii) obtain one method for the generation of all the possible local configurations corresponding to the maximum number of neighbours, (iii) determine which of those configurations generate the growth on the generic site i and (iv) minimize the number of rules. Note that the last step is not really necessary.

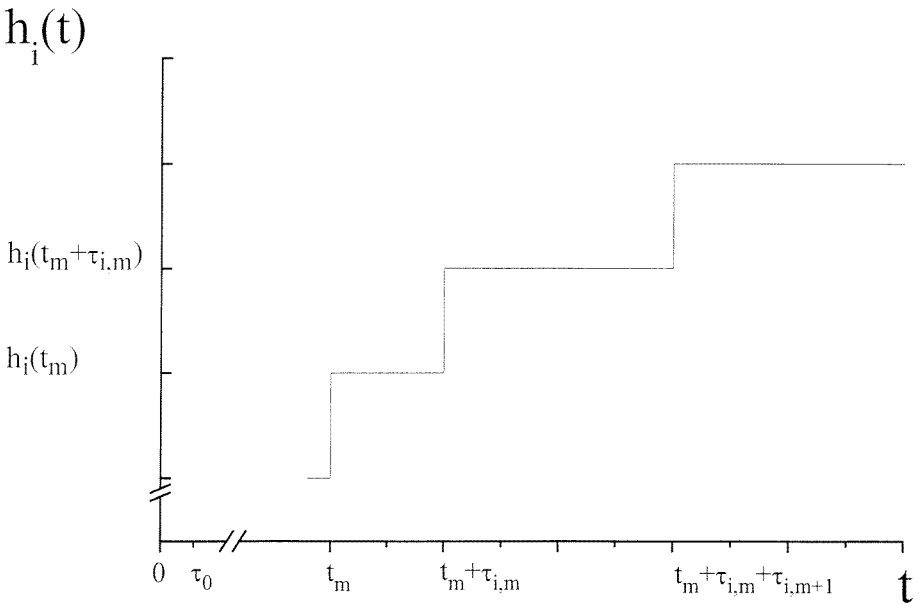

Figure 1. A portion of the $h_i(t)$ plot. It is easy to see that, due to the fact that $h_i(t)$ is constant between two successive depositions, $h_i(t_m + \tau_{i,m} - \tau_0) = h_i(t_m)$.

However, the reduction in the number of microscopic rules facilitates the attainment of the Langevin equations. In order to illustrate the above description we shall obtain the microscopic rules of the DT model (without diffusion) given in [14] in detail.

3.1. DT model (without diffusion)

The DT model without diffusion has been studied in [14], where five microscopic rules were given to define the model. Due to the fact that the falling particle remains in the randomly chosen site or relaxes to one of the two neighbours, the maximum number of particles involved in this model is three. On the other hand, the relaxation depends on whether the height differences of two nearest neighbours $h_k - h_l$ is bigger, smaller than or equal to zero ($h_k - h_l > 0$, $h_k - h_l < 0$ or $h_k - h_l = 0$). Then, for this model there are two steps between the three particles involved and nine possible local configurations per site (see figure 2). The other 18 configurations can be obtained making the substitution $i \to i-1$ in the nine rules given in figure 2 generating the rules $r_{10}, \ldots, r_{18}$ and making the substitution $i \to i+1$ the last nine configurations $r_{19}, \ldots, r_{27}$ are obtained and complete the configurations that define this model. It is easy to see that the definition of a model in this graphical representation is achieved given the site where the falling particle deposits in each of the 27 elementary local configurations.

Let us first define the height difference H_l^k between two sites k and l at time $t + \tau_{i,n} - \tau_0$ as

$$H_l^k = h_k(t + \tau_{i,n} - \tau_0) - h_l(t + \tau_{i,n} - \tau_0). \tag{4}$$

After expanding H_l^k in a Taylor series about t and retaining the first term, we obtain

$$H_l^k = h_k(t) - h_l(t) + \mathrm{O}(\tau_{i,n} - \tau_0) \tag{5}$$

which is an approximation that will be used throughout this paper.

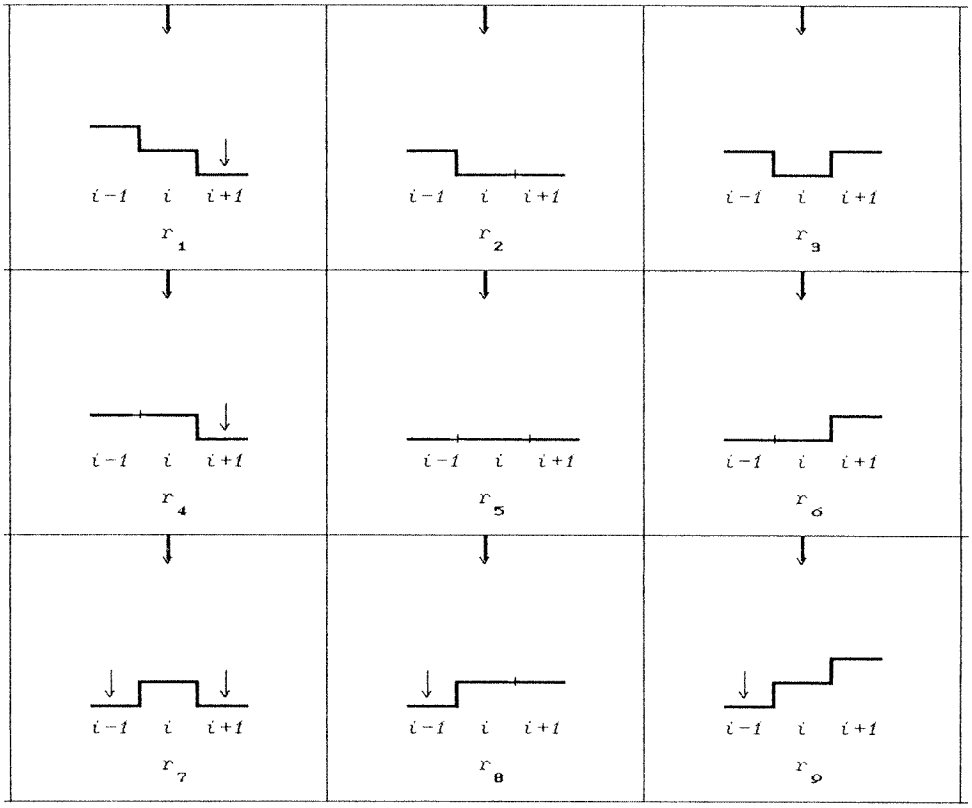

Figure 2. The nine elementary local configurations generated by a particle falling on site i for the DT model. The upper arrow indicates the randomly chosen site j and the lower the possible sites where the falling particles relax or diffuse.

The analytical expression of the four elementary rules that generate a growth on site i due to a particle falling on site i are

$$r_2 = a[\delta_{i,j}\theta^*(H_i^{i-1})\delta(h_i, h_{i+1})] \tag{6}$$

$$r_3 = a[\delta_{i,j}\theta^*(H_i^{i-1})\theta^*(H_i^{i+1})] \tag{7}$$

$$r_5 = a[\delta_{i,j}\delta(h_i, h_{i-1})\delta(h_i, h_{i+1})] \tag{8}$$

and

$$r_6 = a[\delta_{i,j}\delta(h_{i-1}, h_i)\theta^*(H_i^{i+1})] \tag{9}$$

where a is the lattice constant, $\delta_{k,l}$ or $\delta(h_k, h_l)$ is the Kronecker symbol, $\theta(y)$ is the step function and $\theta^*(y) = 1 - \theta(-y)$ for any k, l and y. In this paper we use the most compact notation $\delta_{k,l}$ instead of $\delta(x_k, x_l)$ according to that used in [14] with the hope that this causes no confusion.

Adding equations (6) and (7) and using equation (103) of the appendix, we obtain

$$r_2 + r_3 = a[\delta_{i,j}\theta^*(H_i^{i-1})\theta(H_i^{i+1})] \tag{10}$$

similarly,

$$r_5 + r_6 = a[\delta_{i,j}\delta(h_{i-1}, h_i)\theta(H_i^{i+1})]. \tag{11}$$

Finally, applying the same procedure to equations (10) and (11), we obtain

$$r_2 + r_3 + r_5 + r_6 = a[\delta_{i,j}\theta(H_i^{i-1})\theta(H_i^{i+1})]. \tag{12}$$

This is the analytical expression for the rule r_1 obtained in [14].

In the same way the elementary rules generated by a particle falling on site $i-1$ and relaxing to site i are the three shown in figure 2 (after replacing i by $i-1$) and the analytical expressions are

$$r_{10} = a[\delta_{i-1,j}\theta^*(H_{i-1}^{i-2})\theta^*(H_i^{i-1})] \tag{13}$$

$$r_{14} = a[\delta_{i-1,j}\delta(h_{i-2}, h_{i-1})\theta^*(H_i^{i-1})] \tag{14}$$

and

$$r_{16} = \tfrac{1}{2}a[\delta_{i-1,j}\theta(H_{i-2}^{i-1})\theta^*(H_i^{i-1})]. \tag{15}$$

Adding equations (13) and (14) and using equation (103) in the appendix, we obtain

$$r_{10} + r_{14} = a[\delta_{i-1,j}\theta^*(H_i^{i-1})\theta(H_{i-1}^{i-2})]. \tag{16}$$

This is the analytical expression for rule r_2 in [14] and r_{16} is the same as r_3 as we expected.

Finally, the elementary rules corresponding to the relaxation of one particle falling on site $i+1$ and producing a growth in site i are the three shown in figure 2 after replacing i by $i+1$ in all the rules. The analytical expressions are

$$r_{25} = \tfrac{1}{2}a[\delta_{i+1,j}\theta^*(H_i^{i+1})\theta^*(H_{i+2}^{i+1})] \tag{17}$$

$$r_{26} = a[\delta_{i1,j}\delta(h_{i+2}, h_{i+1})\theta^*(H_i^{i+1})] \tag{18}$$

and

$$r_{27} = a[\delta_{i+1,j}\theta(H_{i+1}^{i+2})\theta^*(H_i^{i+1})]. \tag{19}$$

Adding equations (18) and (19) and using equation (103) of the appendix, we obtain

$$r_{25} + r_{26} = a[\delta_{i+1,j}\theta^*(H_i^{i+1})\theta(H_{i+1}^{i+2})]. \tag{20}$$

This is the analytical expression for the rule r_4. On the other hand r_{27} is the same as r_5 and completes the five rules given in [14].

This example shows the basic aspects of obtaining the growth rules of a given model from the elementary local configurations. It is easy to see that the set of rules needed to describe a model is not unique and we can use alternatively the 10 elementary rules given above or the five microscopic rules given in [14]. The use of the summation procedure given in the appendix is extremely useful and simplifies considerably the work needed to deduce the Langevin equations.

4. Das Sarma–Tamborenea model

In this section we apply our procedure to obtain the Langevin equation from the elementary relaxation and diffusion mechanisms of the DT model.

Now, we must derive explicitly the rules given in equation (3) for the DT model. In this model with relaxation and diffusion the maximum number of sites involved are five and the number of steps four. As we have shown in the previous example each step can be in three 'states' and the number of elementary local configurations is $3^4 = 81$ per site, then the growth of the generic site i due to particles falling on sites $i, i-1$ and $i+1$ will give a total of 243 elementary local configurations. Using repeatedly the summation rules given in the appendix and after tedious but simple deductions as in the previous section,

the growth rules for the site i (see figure 3) can be obtained. Avoiding the generation of the 243 elementary local configurations and the reduction to the microscopic rules given in figure 3, we proceed straightforwardly to give the analytical expressions for the microscopic rules.

Let us first write equation (3) as

$$h_i(t+\tau_{i,n}) = h_i(t) + r_1 + r_2 + \cdots + r_{16} \tag{21}$$

where the elementary rules $r_1, \ldots, r_{16}$ can be written analytically as

$$r_1 = a[\delta_{i,j}\theta(H_{i-2}^{i-1})\delta(h_i, h_{i-1})\delta(h_{i+1}, h_i)\theta(H_{i+2}^{i+1})] \tag{22}$$

$$r_2 = a[\delta_{i,j}\theta^*(H_i^{i-1})\theta(H_{i+1}^{i})] \tag{23}$$

$$r_3 = a[\delta_{i,j}\theta^*(H_i^{i-1})\theta^*(H_i^{i+1})] \tag{24}$$

$$r_4 = a[\delta_{i,j}\theta(H_{i-1}^{i})\theta^*(H_i^{i+1})] \tag{25}$$

$$r_5 = a[\delta_{i+1,j}\theta^*(H_i^{i-1})\delta(h_{i+1}, h_i)\delta(h_{i+2}, h_{i+1})\theta(H_{i+3}^{i+2})] \tag{26}$$

$$r_6 = \tfrac{1}{2}a[\delta_{i+1,j}\theta^*(H_i^{i-1})\delta(h_{i+1}, h_i)\delta(h_{i+2}, h_{i+1})\theta^*(H_{i+2}^{i+3})] \tag{27}$$

$$r_7 = a[\delta_{i+1,j}\theta^*(H_i^{i+1})\delta(h_{i+2}, h_{i+1})\theta(H_{i+3}^{i+2})] \tag{28}$$

$$r_8 = \tfrac{1}{2}a[\delta_{i+1,j}\theta^*(H_i^{i+1})\delta(h_{i+2}, h_{i+1})\theta^*(H_{i+2}^{i+3})] \tag{29}$$

$$r_9 = \tfrac{1}{2}a[\delta_{i+1,j}\theta^*(H_i^{i-1})\delta(h_{i+1}, h_i)\theta^*(H_{i+2}^{i+1})] \tag{30}$$

$$r_{10} = \tfrac{1}{2}a[\delta_{i+1,j}\theta^*(H_i^{i+1})\theta^*(H_{i+2}^{i+1})] \tag{31}$$

$$r_{11} = a[\delta_{i-1,j}\theta(H_{i-3}^{i-2})\delta(h_{i-1}, h_{i-2})\delta(h_i, h_{i-1})\theta^*(H_i^{i+1})] \tag{32}$$

$$r_{12} = \tfrac{1}{2}a[\delta_{i-1,j}\theta^*(H_{i-2}^{i-3})\delta(h_{i-1}, h_{i-2})\delta(h_i, h_{i-1})\theta^*(H_i^{i+1})] \tag{33}$$

$$r_{13} = a[\delta_{i-1,j}\theta(H_{i-3}^{i-2})\delta(h_{i-1}, h_{i-2})\theta^*(H_i^{i-1})] \tag{34}$$

$$r_{14} = \tfrac{1}{2}a[\delta_{i-1,j}\theta^*(H_{i-2}^{i-3})\delta(h_{i-1}, h_{i-2})\theta^*(H_i^{i-1})] \tag{35}$$

$$r_{15} = \tfrac{1}{2}a[\delta_{i-1,j}\theta^*(H_{i-2}^{i-1})\delta(h_i, h_{i-1})\theta^*(H_i^{i+1})] \tag{36}$$

$$r_{16} = \tfrac{1}{2}a[\delta_{i-1,j}\theta^*(H_{i-2}^{i-1})\theta^*(H_i^{i-1})] \tag{37}$$

and $h_i(t+\tau_{i,n}-\tau_0) = h_i(t)$ was used (see figure 1).

In order to compare the results of this section with the results of [15] let us write equation (3) as

$$h_i(t+\tau_{i,n}) = h_i(t) + a(\delta_{i,j}w_i + \delta_{i+1,j}w_{i+1} + \delta_{i-1,j}w_{i-1}) \tag{38}$$

where

$$w_i = r_1^{(1)} + \cdots + r_4^{(1)} \tag{39}$$

$$w_{i+1} = r_5^{(2)} + \cdots + r_{10}^{(2)} \tag{40}$$

$$w_{i-1} = r_{11}^{(3)} + \cdots + r_{16}^{(3)} \tag{41}$$

and

$$r_l^{(1)} = \frac{r_l}{\delta_{i,j}} \qquad \text{for } l = 1, \ldots, 4 \tag{42}$$

$$r_l^{(2)} = \frac{r_l}{\delta_{i+1,j}} \qquad \text{for } l = 5, \ldots, 10 \tag{43}$$

$$r_l^{(3)} = \frac{r_l}{\delta_{i-1,j}} \qquad \text{for } l = 11, \ldots, 16. \tag{44}$$

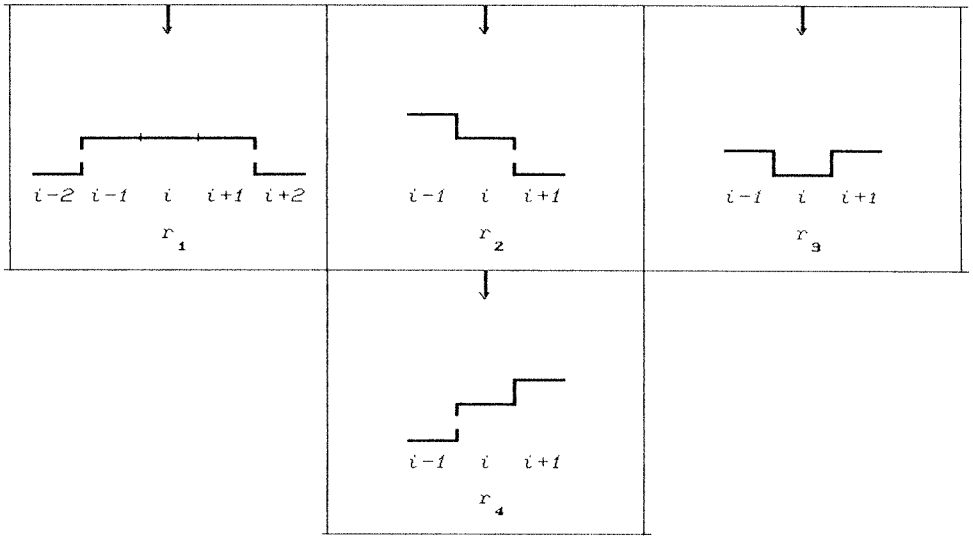

Figure 3. The 16 graphical representations corresponding to the rules $r_1, \ldots, r_{16}$ of the DT model indicating all the possible situations for the growth of site i. The upper arrow indicates the randomly chosen site j and the lower the possible sites where the falling particles relax or diffuse. The broken vertical segments between two nearest neighbours k and l indicate that $h_k \geqslant h_l$ and the full ones that $h_k > h_l$. (*a*) The four rules for the situation where the particle falls on site i. (*b*) The six rules corresponding to the situation where the particle falls on site $i+1$. (*c*) The six rules corresponding to the situation where the particle falls on site $i-1$. It is interesting to observe that the rules of (*c*) are the specular image of those shown in (*b*).

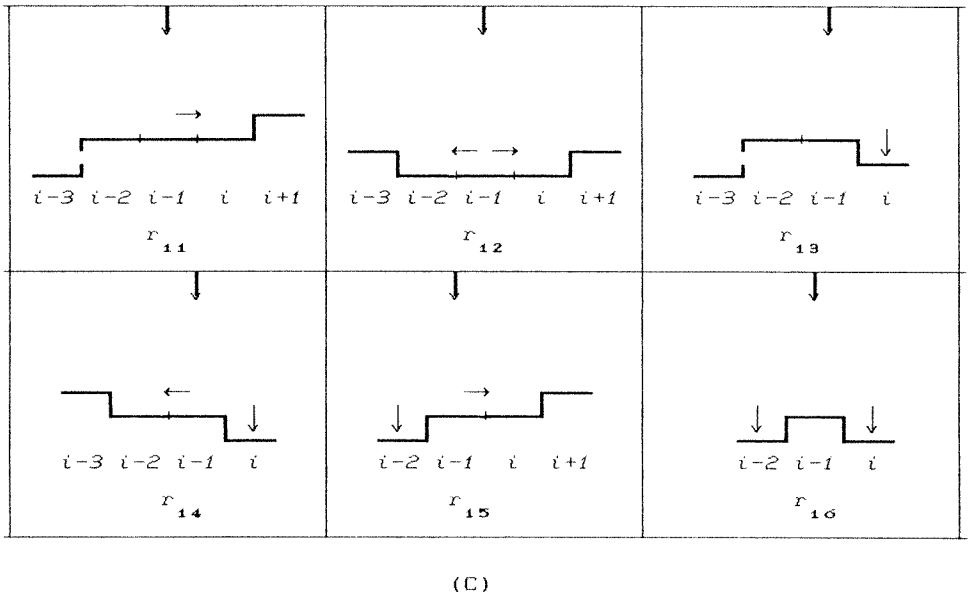

Figure 3. (Continued)

Expanding $h_i(t+\tau_{i,n})$ in a Taylor series and retaining the first two terms, equation (6) can be written as

$$\frac{\mathrm{d}h_i(t)}{\mathrm{d}t}\tau_{i,n} = a(\delta_{i,j}w_i + \delta_{i+1,j}w_{i+1} + \delta_{i-1,j}w_{i-1}). \tag{45}$$

Expanding the Kronecker symbols in a Taylor series as in appendix A of [14] we easily find

$$\delta_{i,j} = 1 + \eta_i(x_j) + \eta_i(x_i) \tag{46}$$

$$\delta_{i+1,j} = 1 + \eta_{i+1}(x_j) + \eta_{i+1}(x_{i+1}) \tag{47}$$

$$\delta_{i-1,j} = 1 + \eta_{i-1}(x_j) + \eta_{i-1}(x_{i-1}) \tag{48}$$

and splitting $\tau_{i,n}$ as in equation (2) we obtain

$$\frac{\mathrm{d}h_i(t)}{\mathrm{d}t} = \frac{a}{\tau}(w_i + w_{i+1} + w_{i-1}) + \eta. \tag{49}$$

Here the sum of the right-hand side is exactly the first transition moment obtained by Zhi-Feng Huang *et al* in [15] and the remainder term η can be written as (see appendix A in [14]):

$$\eta = \eta_0 + \eta_s + \eta_d \tag{50}$$

where

$$\eta_0 = -\frac{\mathrm{d}h_i(t)}{\mathrm{d}t}\frac{\delta\tau_{i,n}}{\tau} \tag{51}$$

$$\eta_s = \frac{\eta_i(x_j)w_i + \eta_{i+1}(x_j)w_{i+1} + \eta_{i-1}(x_j)w_{i-1}}{\tau} \tag{52}$$

and

$$\eta_d = \frac{\eta_i(x_i)w_i + \eta_{i+1}(x_{i+1})w_{i+1} + \eta_{i-1}(x_{i-1})w_{i-1}}{\tau}. \tag{53}$$

Finally, after using the results given in appendix B of [14] consisting in replacing $h_i(t)$ by an interpolating function $h(x_i, t)$, expanding all the Kronecker symbols and step functions in a Taylor series retaining terms up to $A_2(H_l^k)^2$ and expanding H_l^k in a Taylor series up to $O(a^5)$, we can easily find the continuum growth equation of the Langevin type corresponding to the DT model, namely

$$\frac{\partial h(x_i,t)}{\partial t} = \left[F - \nu_4 \frac{\partial^4 h(x_i,t)}{\partial x_i^4} + \lambda_{22} \frac{\partial^2}{\partial x_i^2} \left(\frac{\partial h(x_i,t)}{\partial x_i} \right)^2 \right] + \eta \tag{54}$$

where

$$F = \frac{a}{\tau} \tag{55}$$

$$\nu_4 = \frac{a^5}{\tau} A_1 \tag{56}$$

$$\lambda_{22} = \frac{a^5}{\tau}(-A_1^2 + 2A_2) \tag{57}$$

in complete agreement with equations (23) and (24) of [15] as we expected.

During the derivation of the Langevin equation we neglect the products A_2A_1 and A_2A_2 and consequently $\theta^*(H_l^k)\delta(h_m, h_n) \approx \theta^*(H_l^k)$ for any k, l, m and n. This approximation simplifies enormously the tedious but simple calculations.

5. Wolf–Villain model

This model is defined by the following rules shown graphically in figure 4

$$h_i(t + \tau_{i,n}) = h_i(t) + r_1 + r_2 + \cdots + r_{25} \tag{58}$$

where the analytic expressions for the 25 rules are

$$r_1 = a[\delta_{i,j}\theta H_{i-2}^{i-1})\delta(h_i, h_{i-1})\delta(h_{i+1}, h_i)\theta(H_{i+2}^{i+1})] \tag{59}$$

$$r_2 = a[\delta_{i,j}\theta(H_i^{i-1})\theta(H_i^{i+1})] \tag{60}$$

$$r_3 = -a[\delta_{i,j}\delta(h_{i-1}, h_i)\delta(h_{i+1}, h_i)] \tag{61}$$

$$r_4 = a[\delta_{i,j}\theta^*(H_i^{i-1})\theta^*(H_{i+1}^i)\theta(H_{i+2}^{i+1})] \tag{62}$$

$$r_5 = a[\delta_{i,j}\theta(H_{i-2}^{i-1})\theta^*(H_{i-1}^i)\theta^*(H_i^{i+1})] \tag{63}$$

$$r_6 = a[\delta_{i+1,j}\theta^*(H_i^{i-1})\delta(h_{i+1}, h_i)\delta(h_{i+2}, h_{i+1})\theta(H_{i+3}^{i+2})] \tag{64}$$

$$r_7 = \tfrac{1}{2}a[\delta_{i+1,j}\theta^*(H_i^{i-1})\delta(h_{i+1}, h_i)\delta(h_{i+2}, h_{i+1})\theta^*(H_{i+2}^{i+3})] \tag{65}$$

$$r_8 = a[\delta_{i+1,j}\theta^*(H_i^{i+1})\delta(h_{i+2}, h_{i+1})\theta(H_{i+3}^{i+2})] \tag{66}$$

$$r_9 = a[\delta_{i+1,j}\theta^*(H_i^{i-1})\theta^*(H_i^{i+1})\delta(h_{i+2}, h_{i+1})\theta^*(H_{i+2}^{i+3})] \tag{67}$$

$$r_{10} = \tfrac{1}{2}a[\delta_{i+1,j}\theta(H_{i-1}^i)\theta^*(H_i^{i+1})\delta(h_{i+2}, hi+1)\theta^*(H_{i+2}^{i+3})] \tag{68}$$

$$r_{11} = \tfrac{1}{2}a[\delta_{i+1,j}\theta^*(H_i^{i-1})\delta(h_{i+1}, h_i)\theta^*(H_{i+2}^{i+1})\theta(H_{i+3}^{i+2})] \tag{69}$$

$$r_{12} = a[\delta_{i+1,j}\theta^*(H_i^{i-1})\theta^*(H_i^{i+1})\theta^*(H_{i+2}^{i+1})\theta(H_{i+3}^{i+2})] \tag{70}$$

$$r_{13} = \tfrac{1}{2}a[\delta_{i+1,j}\theta(H_{i-1}^i)\theta^*(H_i^{i+1})\theta^*(H_{i+2}^{i+1})\theta(H_{i+3}^{i+2})] \tag{71}$$

$$r_{14} = \tfrac{1}{2}a[\delta_{i+1,j}\theta^*(H_i^{i-1})\theta^*(H_i^{i+1})\theta^*(H_{i+2}^{i+1})\theta^*(H_{i+2}^{i+3})] \tag{72}$$

$$r_{15} = a[\delta_{i+1,j}\theta^*(H_i^{i-1})\theta^*(H_i^{i+1})\theta^*(H_{i+1}^{i+2})] \tag{73}$$

$$r_{16} = a[\delta_{i-1,j}\theta(H_{i-3}^{i-2})\delta(h_{i-1}, h_{i-2})\delta(h_i, h_{i-1})\theta^*(H_i^{i+1})] \tag{74}$$

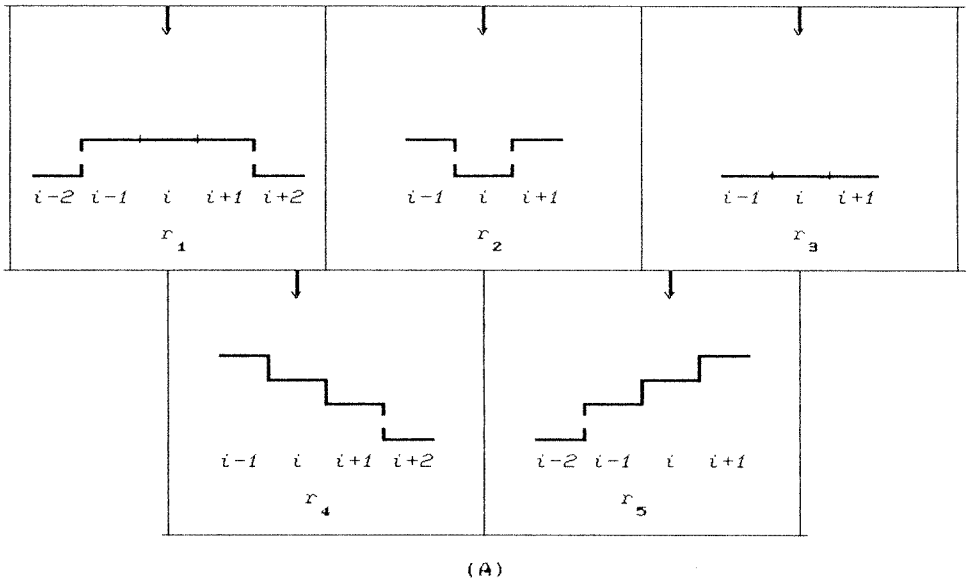

Figure 4. The 25 graphical representations corresponding to the rules $r_1, \ldots, r_{25}$ of the WV model indicating all the possible situations for the growth of the site i. The upper arrow indicates the randomly chosen site j and the lower the possible sites where the falling particles relax or diffuse. (*a*) The five rules for the situation where the particle falls on site i. (*b*) The 10 rules corresponding to the situation where the particle falls on site $i+1$. (*c*) The 10 rules corresponding to the situation where the particle falls on site $i-1$. (*d*) The three rules equivalent to r_2 and r_3 in (*a*). It is interesting to observe that in this model the rules in (*c*) are again the specular image of those shown in (*b*).

$$r_{17} = \tfrac{1}{2}a[\delta_{i-1,j}\theta^*(H_{i-2}^{i-3})\delta(h_{i-1}, h_{i-2})\delta(h_i, h_{i-1})\theta^*(H_i^{i+1})] \tag{75}$$

$$r_{18} = a[\delta_{i-1,j}\theta(H_{i-3}^{i-2})\delta(h_{i-1}, h_{i-2})\theta^*(H_i^{i-1})] \tag{76}$$

$$r_{19} = \tfrac{1}{2}a[\delta_{i-1,j}\theta(H_{i-3}^{i-2})\theta^*(H_{i-2}^{i-1})\delta(h_i, h_{i-1})\theta^*(H_i^{i+1})] \tag{77}$$

$$r_{20} = a[\delta_{i-1,j}\theta^*(H_{i-2}^{i-3})\delta(h_{i-1}, h_{i-2})\theta^*(H_i^{i-1})\theta^*(H_i^{i+1})] \tag{78}$$

$$r_{21} = \tfrac{1}{2}a[\delta_{i-1,j}\theta^*(H_{i-2}^{i-3})\delta(h_{i-1}, h_{i-2})\theta^*(H_i^{i-1})\theta(H_{i+1}^{i})] \tag{79}$$

$$r_{22} = \tfrac{1}{2}a[\delta_{i-1,j}\theta(H_{i-3}^{i-2})\theta^*(H_{i-2}^{i-1})(H_i^{i-1})\theta^*(H_i^{i+1})] \tag{80}$$

$$r_{23} = \tfrac{1}{2}a[\delta_{i-1,j}\theta(H_{i-3}^{i-2})\theta^*(H_{i-2}^{i-1})\theta^*(H_i^{i-1})\theta(H_{i+1}^{i})] \tag{81}$$

$$r_{24} = \tfrac{1}{2}a[\delta_{i-1,j}\theta^*(H_{i-2}^{i-3})\theta^*(H_{i-2}^{i-1})\theta^*(H_i^{i-1})\theta^*(H_i^{i+1})] \tag{82}$$

$$r_{25} = a[\delta_{i-1,j}\theta^*(H_{i-1}^{i-2})\theta^*(H_i^{i-1})\theta^*(H_i^{i+1})]. \tag{83}$$

In the same way as in the previous section

$$w_i = r_1^{(1)} + \cdots + r_5^{(1)} \tag{84}$$

$$w_{i+1} = r_6^{(2)} + \cdots + r_{15}^{(2)} \tag{85}$$

$$w_{i-1} = r_{16}^{(3)} + \cdots + r_{25}^{(3)} \tag{86}$$

and

$$r_l^{(1)} = \frac{r_l}{\delta_{i,j}} \qquad \text{for } l = 1, \ldots, 5 \tag{87}$$

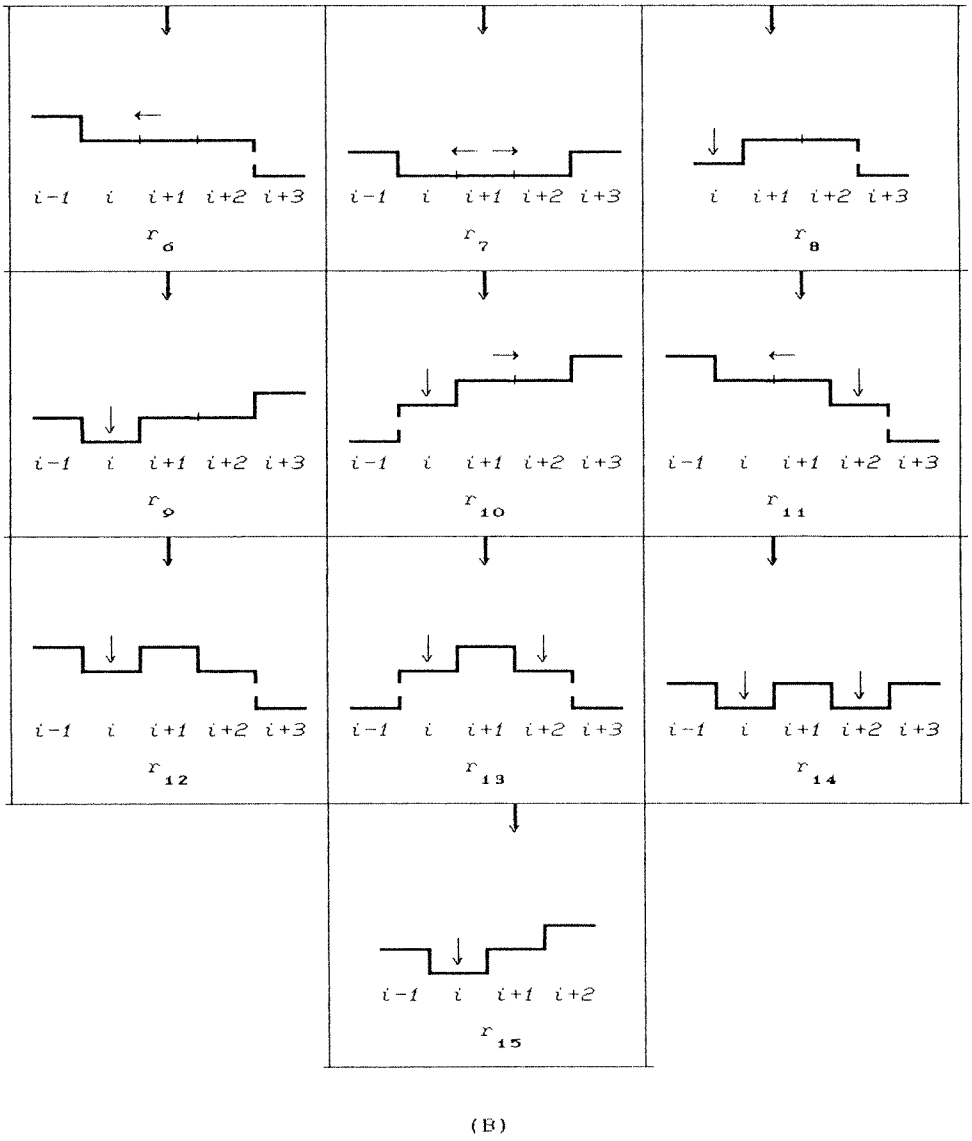

Figure 4. (Continued)

$$r_l^{(2)} = \frac{r_l}{\delta_{i+1,j}} \qquad \text{for } l = 6, \ldots, 15 \tag{88}$$

$$r_l^{(3)} = \frac{r_l}{\delta_{i-1,j}} \qquad \text{for } l = 16, \ldots, 25. \tag{89}$$

Replacing w_i, w_{i-1} and w_{i+1} in equations (45)–(53) the first transition moment, the discrete Langevin equation and η are straightforwardly evaluated.

Defining an interpolating function for the height profile, expanding as in the previous section all the functions in a Taylor series and retaining terms up to $O(a^5)$, the corresponding

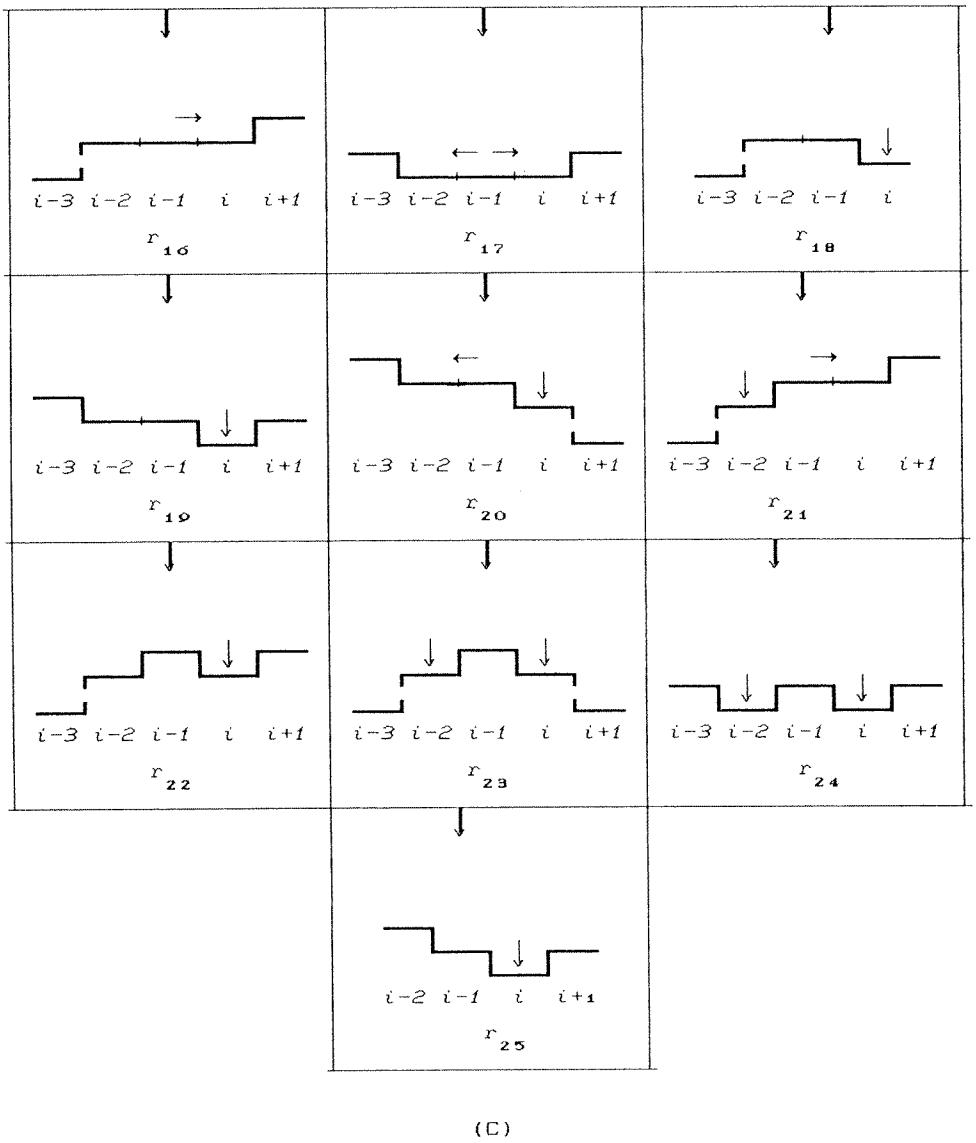

(C)

Figure 4. (Continued)

continuum Langevin equation for the WV model is

$$\frac{\partial h(x_i,t)}{\partial t} = \left[F - \nu_4 \frac{\partial^4 h(x_i,t)}{\partial x_i^4} + \lambda_{22} \frac{\partial^2}{\partial x_i^2} \left(\frac{\partial h(x_i,t)}{\partial x_i} \right)^2 - \lambda_{13} \frac{\partial}{\partial x_i} \left(\frac{\partial h(x_i,t)}{\partial x_i} \right)^3 \right] + \eta \quad (90)$$

where

$$F = \frac{a}{\tau} \quad (91)$$

$$\nu_4 = \frac{a^5}{\tau} A_1 \quad (92)$$

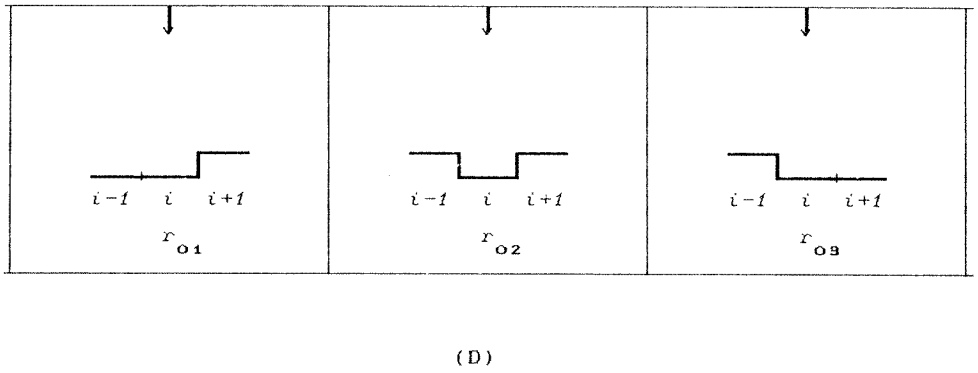

Figure 4. (Continued)

$$\lambda_{22} = \frac{a^5}{\tau}(-A_1^2 + 2A_2) \tag{93}$$

$$\lambda_{13} = -\frac{2a^5}{\tau}A_1^3. \tag{94}$$

After the 243 elementary local configurations corresponding to this model are reduced using the summation rules given in the appendix, we obtain r_1, r_4, r_5 and the three rules given in figure 4(d). It is not difficult to show that the sum of the three rules given in figure 4(d) are equal to the sum of the rules r_2 and r_3 given in figure 4(a). The demonstration is based on equation (103) given in the appendix. Let us write r_2 as

$$r_2 = a\delta_{i,j}[\theta^*(H_i^{i-1}) + \delta(h_{i-1}, h_i)][\theta^*(H_i^{i+1}) + \delta(h_i, h_{i+1})]. \tag{95}$$

Expanding the product in the right-hand side it is easy to see that

$$r_2 = -r_3 + r_{01} + r_{02} + r_{03} \tag{96}$$

and then the sum of the two rules $(r_2 + r_3)$ given in figure 4(a) is equal to the sum of the three rules $(r_{01} + r_{02} + r_{03})$ given in figure 4(d).

6. Conclusions

The two discrete models discussed in this paper are probably the most studied models of molecular-beam epitaxy and were introduced by DT and WV in order to mimic surface growth processes with deposition and surface diffusion. The general procedure of deriving continuum Langevin equations directly from the growth rules, avoiding the complications arising in the master equation approach, was used and compared with the previous results obtained in [15]. Our method is considerably simpler and more intuitive than the master equation approach and the generalization to higher dimensions is straightforward. This generalization is of great importance not just for pure theoretical reasons but for the fact that simulations on two-dimensional systems are extremely time-consuming. It is interesting to note that the number of microscopic rules corresponding to the DT and WV models are considerably larger than the two models studied in [14] and the reasons are the inclusion of the surface diffusion and the fact that the relaxation depends on the next-nearest neighbours in these models. On the other hand the concept of elementary local configurations was developed in section 3 and the microscopic rules were derived using simple summation rules. An isomorphism between the analytical and the graphical representations was established in

the appendix allowing a rigorous passage from one representation to the other. In conclusion, the method for the construction of the Langevin equations developed in [14] shows that the discrete model approach is considerably easier and more intuitive than the equivalent master equation approach. The concept of elementary local configurations allows the derivation of the microscopic rules and demonstrates that the set of rules used in the definition of a given model is not unique and the use of the simplest set is convenient but not necessary. Finally, the summation rules allow the connection of two sets of rules and give a tool to determine whether both sets belong to the same model or not.

Appendix

A.1. Graphic–analytic equivalence

The equivalence between the graphical and the analytical representation of the growth rules used to describe a given model can be reduced to the following six, needed to compare the height difference between two nearest neighbours k and l

$\theta(H_l^k) =$ 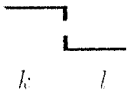

(97)

$\theta(H_k^l) =$ 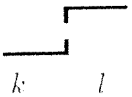

(98)

$\delta(h_k, h_l) =$ 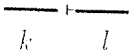

(99)

$\theta^*(H_l^k) =$ 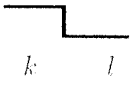

(100)

$\theta^*(H_k^l) =$ 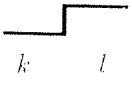

(101)

$$\downarrow$$

$$\delta_{i+\alpha,j} = \iota + \alpha \qquad \text{for } \alpha = -1, 0, 1. \tag{102}$$

With the six definitions given above it is easy to generate more complex rules consisting in products of the analytical elementary rules and the equivalent graphical representation consisting in putting the elementary graphs in a sequence such as those shown in figures 2–4. Vice versa, given a graph consisting in a sequence of elementary graphs we can find the analytical representation writing the corresponding products (one per pair of nearest-neighbour sites) of elementary rules.

A.2. Useful summation rules

Two useful relations between the elementary rules that are needed to reduce the number of graphs and the length of a given graph are

$$\theta(H_l^k) = \theta^*(H_l^k) + \delta(h_k, h_l) \tag{103}$$

and

$$\theta^*(H_l^k) + \theta^*(H_k^l) + \delta(h_k, h_l) = 1. \tag{104}$$

The rule given in equation (103) was used in section 3 in the process of reducing the elementary rules for the DT model without diffusion to the five microscopic rules given in [14]. Let us show an example where the rule given in equation (104) is used. The rule r_8 shown in figure 3(b) is the sum of the following three

$$r_{81} = \tfrac{1}{2}a[\delta_{i+1,j}\theta^*(H_{i-1}^{i})\theta^*(H_i^{i+1})\delta(h_{i+2},h_{i+1})\theta^*(H_{i+2}^{i+3})] \tag{105}$$

$$r_{82} = \tfrac{1}{2}a[\delta_{i+1,j}\delta(h_{i-1},h_i)\theta^*(H_i^{i+1})\delta(h_{i+2},h_{i+1})\theta^*(H_{i+2}^{i+3})] \tag{106}$$

and

$$r_{83} = \tfrac{1}{2}a[\delta_{i+1,j}\theta^*(H_i^{i-1})\theta^*(H_i^{i+1})\delta(h_{i+2},h_{i+1})\theta^*(H_{i+2}^{i+3})]. \tag{107}$$

The graphical representation of rules r_{81}, r_{82} and r_{83} is the same as graph r_8 in figure 3(b) with an extra step between $i-1$ and i corresponding to the three elementary rules $\theta^*(H_{i-1}^{i})$, $\delta(h_{i-1},h_i)$ and $\theta^*(H_i^{i-1})$ respectively.

Acknowledgments

The author wishes to acknowledge the Departamento de Física and the members of the Grupo de Físicoquimica de Superficies, specially Dr Victor Pereyra and Professor T P Eggarter for valuable suggestions and in a revised version Professor G Zgrablich carefully read the manuscript and numerous spelling and grammatical mistakes were corrected.

References

[1] Barabasi A-L and Stanley H E 1995 *Fractal Concepts in Surface Growth* (New York: Cambridge University Press)
[2] Krug J and Spohn H 1991 *Solids Far From Equilibrium: Growth, Morphology and Defects* ed C Godreche (New York: Cambridge University Press)
Krug J and Spohn H 1991 *Dynamics of Fractal Surfaces* ed F Family and T Vicsek (Singapore: World Scientific)
[3] Herman M A and Sitter H 1989 *Molecular Beam Epitaxy: Fundamentals and Currents Status* (Berlin: Springer)
[4] Das Sarma S and Tamborenea P 1991 *Phys. Rev. Lett.* **66** 325
[5] Wolf D E and Villain J 1990 *Europhys. Lett.* **13** 389
[6] Das Sarma S and Ghaisas S V 1992 *Phys. Rev. Lett.* **69** 3762
[7] Kotrla M, Levi A C and Smilauer P 1992 *Europhys. Lett.* **20** 25
[8] Krug J, Plischke M and Siegert M 1993 *Phys. Rev. Lett.* **70** 3271
[9] Plischke M, Shore J D, Schroeder M, Siegert M and Wolf D E 1993 *Phys. Rev. Lett.* **71** 2509
[10] Das Sarma S and Ghaisas S V 1993 *Phys. Rev. Lett.* **71** 2510
[11] Smilauer P and Kotrla M 1994 *Phys. Rev.* B **49** 5769
[12] Ryu C S and Kim I M 1995 *Phys. Rev.* E **51** 3069
Ryu C S and Kim I M 1995 *Phys. Rev.* E **52** 2424
[13] Vvdensky D D, Zangwill A, Luse C N and Wilby M R 1993 *Phys. Rev.* E **48** 852
[14] Costanza G 1997 *Phys. Rev.* E **55** 6501
[15] Zhi-Feng Huang and Bing-Lin Gu 1996 *Phys. Rev.* E **54** 5935